

***In vitro* Characterization of Chitosan-Whitlockite Scaffolds for Bone Tissue Engineering Applications**

Annanya Arora¹, Palati Sinduja^{2*}, Saravanan Sekaran³, and Dhanraj Ganapathy³

¹*Department of Pathology, Saveetha Dental College and Hospitals, Saveetha Institute of Medical and Technical Sciences, Saveetha University, Chennai - 600077, Tamil Nadu, India*

²*Department of Oral and Maxillofacial Pathology, Saveetha Dental College and Hospitals, Saveetha Institute of Medical and Technical Sciences, Saveetha University, Chennai - 600077, Tamil Nadu, India*

³*Department of Prosthodontics, Saveetha Dental College and Hospitals, Saveetha Institute of Medical and Technical Sciences, Saveetha University, Chennai - 600077, Tamil Nadu, India*

Abstract

The study explores the development of a Chitosan-Whitlockite (Ch-WH) composite scaffold for bone tissue engineering. Chitosan, a natural polymer, and Whitlockite (WH), a calcium-magnesium phosphate mineral, are combined to leverage their individual properties. The scaffold was synthesized and characterized using X-ray diffraction (XRD) to confirm crystalline structure, Fourier-transform infrared spectroscopy (FTIR) for chemical interactions, scanning electron microscopy (SEM) for surface morphology and porosity, and energy-dispersive X-ray spectroscopy (EDS) to verify elemental composition. In vitro evaluations using human osteoblast-like cells demonstrated strong biocompatibility, with the scaffold supporting cell adhesion, proliferation, and differentiation. The addition of magnesium from Whitlockite enhanced osteoblast activity and bone mineralization. The scaffold also exhibited antibacterial properties, minimizing infection risks. With its biocompatibility, bioactivity, and antibacterial potential, the Ch-WH composite scaffold presents a promising solution for bone tissue engineering, warranting further exploration for clinical applications.

Keywords: *Biocompatible Material, Bone Regeneration, Chitosan, Tissue Engineering, Whitlockite.*

Introduction

Bone fracture healing is a highly complex regenerative process aimed at restoring the bone to its pre-injury state structurally and functionally [1]. Critical-size bone defects (CSBDs) are defined as bone defects that are too large to heal without intervention, and their classification is based on experimental data and clinical observations [2]. Bone type, species, and patient-specific characteristics, including lesion size and volume influence these defects.

Current strategies for treating localized bone defects include the use of autografts, allografts, and technologies like Masquelet

membrane induction and bone transfer [3-6]. While effective, these approaches present limitations, including the need for additional surgeries, longer hospital stays, donor site morbidity, and complications such as stress fractures [7, 8]. In cases where natural healing fails, bone regeneration therapies are required to address abnormalities, fractures, and non-unions. Autografts, which involve transferring the patient's bone to the defect site, and allografts, which use donor bone, remain widely used. Still, these methods are constrained by limited donor availability and the risk of immune rejection. Synthetic bone substitutes, such as ceramics or bioactive glass, offer structural support and simulate

bone, but they frequently lack the biological qualities required for healing [9]. Therefore, developing innovative biomaterials to replace traditional medical techniques has become a research focus in recent years [10].

Tissue-engineered constructs, which combine cells, scaffolds, and growth factors, aim to create bioactive environments conducive to healing. Bone tissue is composed of both inorganic and organic materials, with approximately 65% of its structure consisting of inorganic minerals like calcium phosphate. The main inorganic component of bone is calcium hydroxylapatite [$\text{Ca}_{10}(\text{PO}_4)_6(\text{OH})_2$], a nanocrystalline material. [11, 12]. In addition to calcium and phosphate, trace elements such as carbonate and magnesium also contribute to the bone's composition and are influenced by environmental and dietary factors.

With a weight proportion of 20–35%, whitlockite is a significant inorganic component of bone tissues [13]. Classified as a calcium phosphate, whitlockite is an uncommon mineral. This compound has the formula $\text{Ca}_9\text{Mg}(\text{HPO}_4)(\text{PO}_4)_6$. Whitlockite frequently takes the form of rhombohedral while exhibiting magnesium locations Ca(IV), Ca(V), and HPO_4^{2-} [14]. This rare mineral is found in both natural bone and geological environments, including phosphate rock deposits and meteorites. Despite the challenges associated with synthesizing pure whitlockite, its osteoconductive properties, biocompatibility, and potential for promoting bone cell growth make it a promising candidate for bone tissue engineering applications [15].

Chitosan, a biopolymer derived from the deacetylation of chitin—found in the exoskeletons of crustaceans and cell walls of fungi—is another key material used in tissue engineering. Its chemical structure, composed of β -(1→4)-linked N-acetyl-D-glucosamine and D-glucosamine units, imparts important biological properties such as biodegradability, non-toxicity, and biocompatibility [16-19]. Its

solubility, viscosity, and biological characteristics are all influenced by the degree of deacetylation (DD) [20, 21]. Chitosan's amino groups allow for chemical modifications that enhance its utility across various biomedical applications. In tissue engineering, chitosan promotes tissue regeneration and cell proliferation, making it useful in drug delivery, wound healing, and scaffold construction [22–25]. Due to its similarity to glycosaminoglycans (GAGs), chitosan is particularly effective in replicating the extracellular matrix of bone [26, 27].

The combination of whitlockite's osteoconductive qualities and chitosan's biocompatibility and biodegradability makes a chitosan-whitlockite (CS-WH) scaffold a viable option for bone tissue engineering applications. These scaffolds typically feature an interconnected porous structure that supports nutrient transport, waste removal, and cell infiltration. The size and distribution of pores are critical factors that influence scaffold performance, with the ideal structure maintaining a balance between porosity and mechanical integrity. Chitosan's network of interconnected chains creates the polymeric matrix, while whitlockite particles, incorporated as nanoparticles, reinforce the scaffold by interacting with the chitosan matrix.

Chitosan's positively charged surface facilitates cell adhesion by interacting with the negatively charged components of cell membranes, enhancing cell attachment and proliferation. The fabrication method plays a significant role in determining the final scaffold architecture. Techniques such as solvent casting, particle leaching, and electrospinning yield scaffolds with varying pore sizes, which directly impact cell migration and scaffold strength. Furthermore, the ratio of chitosan to whitlockite affects scaffold properties, with higher chitosan concentrations producing more porous structures and higher whitlockite

concentrations resulting in denser scaffolds. The aim of this work is to analyze the physical, chemical and biological characteristics of a chitosan-whitlockite scaffold and evaluate its potential for bone tissue engineering applications using in vitro analysis.

Materials and Methods

Synthesis of Whitlockite (WH)

To prepare Whitlockite (WH), 25 mL of distilled water was used to dissolve 2.96 grams of calcium nitrate ($\text{Ca}(\text{NO}_3)_2$). In a separate solution, 0.449 grams of magnesium nitrate ($\text{Mg}(\text{NO}_3)_2$) was dissolved in 3.5 mL of distilled water. Both solutions were thoroughly stirred to ensure complete dissolution. Simultaneously, 2.5641 grams of diammonium hydrogen phosphate ($(\text{NH}_4)_2\text{HPO}_4$) were dissolved in 20 mL of deionized water with

gentle stirring. The calcium and magnesium nitrate solutions were slowly added to the diammonium hydrogen phosphate solution under continuous stirring to ensure homogeneity. The pH of the resultant mixture was adjusted to 6 by adding ammonia solution (NH_4OH) while stirring continuously for 1 hour.

The solution was then subjected to autoclaving at 200°C for 15 minutes to facilitate crystallization and composite formation. After autoclaving, the solution was allowed to cool to room temperature. The resulting precipitate was washed thoroughly with ethanol to remove any unreacted components or impurities. The cleaned precipitate was dried overnight to obtain the final calcium-magnesium-phosphate composite. The graphical abstract is represented in Fig.1.

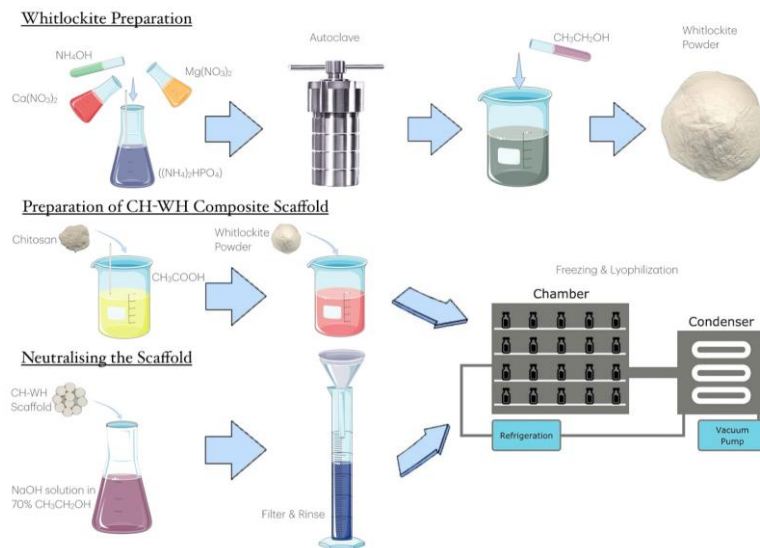


Figure 1. Each part shows a step leading to the formation of WH-CS Scaffold.

Preparation of CH-WH Composite Scaffold

To prepare the CH-WH composite scaffold, 2 grams of chitosan were dissolved in 100 mL of 0.1 M acetic acid solution. The solution was stirred continuously for 2 hours at room temperature to ensure complete dissolution. Once ready, the WH powder was added to the chitosan solution at concentrations of 0.1%, 0.2%, and 0.3%. The mixture was stirred for

an additional 2 hours to achieve uniform dispersion of the WH powder.

The resulting mixture was then frozen at -20°C overnight and lyophilized to produce a dry, porous scaffold.

Neutralization of the Scaffold

To neutralize the scaffold and promote cross-linking of the chitosan, the CH-WH scaffold

was immersed in a 0.5 M NaOH solution prepared with 70% ethanol for 1 hour. Afterward, the scaffold was placed on filter paper to drain excess liquid. It was then thoroughly rinsed with distilled water to remove any residual NaOH and ethanol. The scaffold's pH was checked, and additional rinsing with distilled water was performed if necessary to achieve a pH between 7 and 8. Finally, the scaffold was frozen at -20°C overnight and lyophilized to obtain the CH-WH composite scaffold.

Characterization and Biocompatibility Assessment of the Scaffold

To examine its surface structure, we used Scanning Electron Microscopy (SEM) and energy-dispersive X-ray Spectroscopy (EDS). X-ray Diffraction (XRD) helped us study its crystalline structure, while Fourier Transform Infrared (FTIR) spectroscopy was used to identify key functional groups. To ensure its biocompatibility, we performed an MTT assay with MG-63 cells following the ISO 10993-6:2016 to check for any cytotoxic effects. After 24 hours of incubation for cell attachment, the medium was replaced with treatment medium containing 25, 50, 75 and 100% of the material. The cells were further incubated for another 24 hours to assess cytotoxicity.

Results

XRD Analysis

The X-ray diffraction (XRD) pattern of the chitosan (Ch) sample (black line) exhibits broad peaks (Fig 2(A)), suggesting an amorphous or less crystalline structure. In contrast, the Whitlockite (Wh) sample (red line) displays sharp and intense peaks, confirming a highly crystalline structure. For the composite samples of 1%, 2%, and 3%

Wh-Ch (green, blue, and cyan lines), the diffraction patterns exhibit a gradual shift in peak intensity and position, indicating a progressive reduction in crystallinity as the concentration of Wh increases. This shift signifies an interaction between Wh and Ch, resulting in modified crystallographic properties of the composite materials.

FTIR Analysis

Fourier-transform infrared (FTIR) spectra (Fig 2(B)), provide insights into the functional groups present in the materials. The Ch sample shows a broad absorption band between $3200\text{--}3500\text{ cm}^{-1}$, which can be attributed to O-H or N-H stretching vibrations. Peaks around 2900 cm^{-1} suggest C-H stretching, possibly from aliphatic chains. Additional peaks near $1600\text{--}1650\text{ cm}^{-1}$ correspond to C=O stretching, while N-H bending vibrations appear around 1550 cm^{-1} . For the Wh sample (red line), strong peaks between $1000\text{--}1500\text{ cm}^{-1}$ suggest the presence of C-O, C-N, or C-H bending vibrations. A broad peak around $3200\text{--}3500\text{ cm}^{-1}$ indicates the presence of hydroxyl or amine groups, while sharp peaks around $1700\text{--}1750\text{ cm}^{-1}$ suggest the presence of carboxyl groups. 1% Wh-Ch (green line), 2% Wh-Ch (blue line), and 3% Wh-Ch (cyan line): As the concentration of Wh increases (from 1% to 3%), there are changes in peak intensity and shape, indicating interaction between Wh and Ch components. The combined spectra show shifts and changes in peaks around $3200\text{--}3500\text{ cm}^{-1}$ (O-H/N-H stretching) and in the fingerprint region ($1000\text{--}1500\text{ cm}^{-1}$), suggesting the formation of hydrogen bonds or other interactions. Changes in the intensity of peaks near $1600\text{--}1650\text{ cm}^{-1}$ and $1700\text{--}1750\text{ cm}^{-1}$ could indicate changes in the carbonyl or amide groups due to interaction between Wh and Ch.

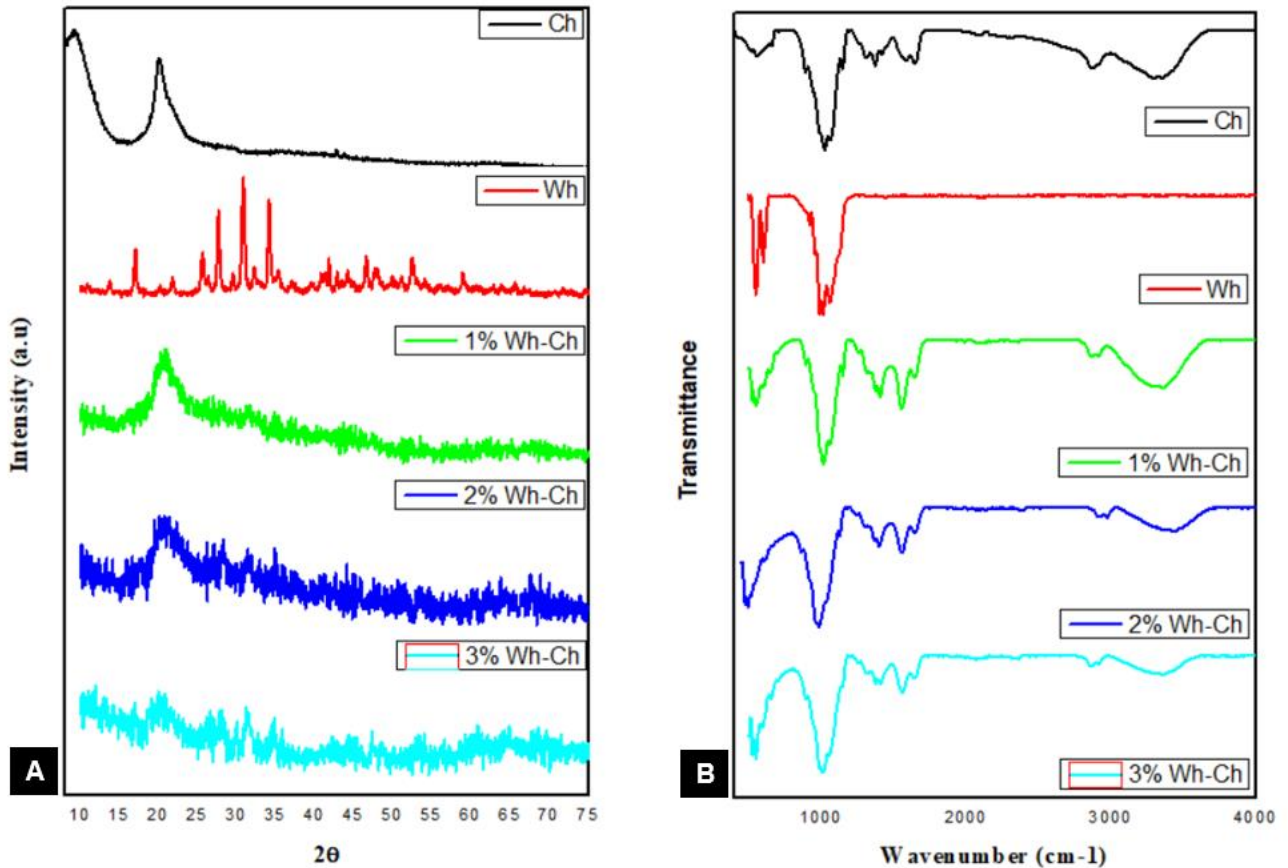


Figure 2. (A) The X-ray diffractogram and (B) shows the FTIR spectra of the representative scaffolds.

SEM Imaging

Scanning electron microscopy (SEM) images (Fig 3) reveal a highly porous structure in the CH-WH scaffold, with interconnected pores of varying sizes. Larger voids are connected by smaller channels, contributing to a rough and irregular surface morphology. The fibrous and sheet-like structures seen in the SEM images suggest a well-integrated scaffold

where chitosan and Whitlockite are homogeneously distributed. The absence of distinct phase separation supports the successful blending of the two materials. The observed morphological characteristics align with the scaffold's potential application in bone tissue engineering, providing a porous network that facilitates cell attachment and nutrient exchange.

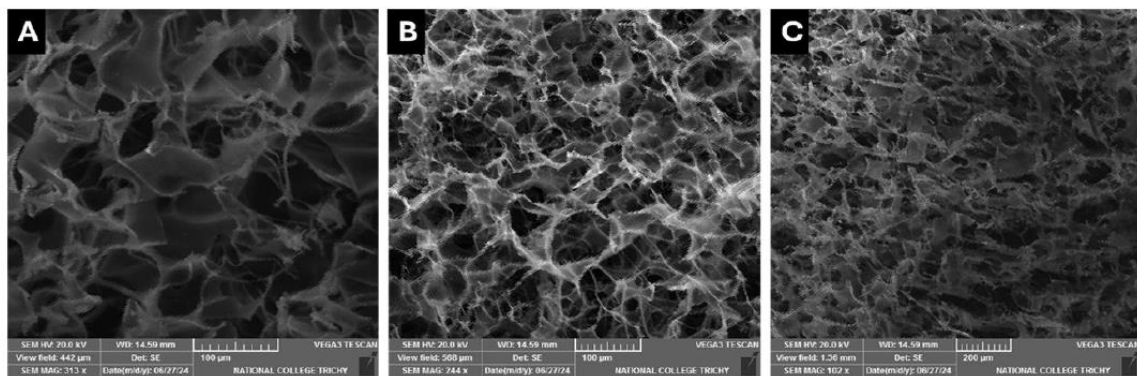


Figure 3. Scanning Electron Microscopic Images of the Whitlockite Incorporated Scaffolds A) 1% Wh- Ch B) 2% Wh- Ch C) 3% Wh- Ch.

EDS Analysis

Energy-dispersive X-ray spectroscopy (EDS) confirms the presence of key elements in the composite material. Carbon (C) and Nitrogen (N) correspond to the chitosan matrix, while Oxygen (O), Phosphorus (P), and Calcium (Ca) are indicative of the Whitlockite component. The detection of Magnesium (Mg) further confirms the chemical composition of Whitlockite, consistent with its known formula, $\text{Ca}_9\text{Mg}(\text{HPO}_4)(\text{PO}_4)_6$. The presence of these elements suggests that the CH-WH composite was synthesized as intended, incorporating both organic (Ch) and inorganic (Wh) phases.

Biocompatibility: MTT Assay

The MTT assay (Fig 4) was employed to evaluate the cytotoxicity and biocompatibility of the CH-WH scaffold on MG-63 cells. The control group exhibited optimal cell viability

at a scaffold concentration of 1% Wg-Ch scaffold. Cell viability remained comparable to the control as the concentration increased to 25% and 50%, indicating minimal cytotoxic effects at these concentrations. However, at 75% and 100% scaffold concentrations, a noticeable reduction in cell viability was observed, suggesting a potential cytotoxic response at higher scaffold concentrations. The viability of cells was observed with scaffold concentrations of 2% Wg-Ch scaffold, where the 25% and 50% and 75% dilutions resulted in peak viability. Interestingly, at a scaffold concentration of 30 mg/mL, the highest cell viability was recorded at the 75% concentration, with diminished viability at higher concentrations. These results suggest that the scaffold exhibits good biocompatibility, with an optimal concentration range of 25-50% for supporting cell proliferation in biomedical applications.

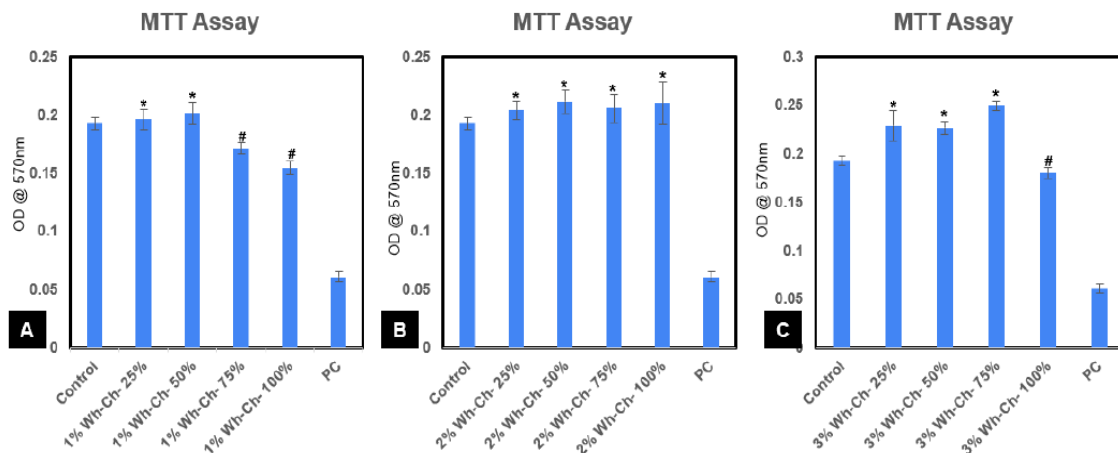


Figure 4: Biocompatibility assessment of the fabricated scaffolds by indirect MTT Assay. A) 1% whitlockite concentration B) 2% whitlockite concentration C) 3% whitlockite concentration. MTT assay results compared the cytotoxicity of scaffolds with the control group, indicating the viability of cells treated with the Whitlockite-Chitosan. Where the * indicates the significantly increased cellular viability of cells compared to the control and the # means the cellular viability is reduced significantly compared to the control.

Discussion

The biological characterization of the chitosan-Whitlockite scaffold highlights its significant potential for use in tissue engineering and regenerative medicine. The combination of Whitlockite (WH), a calcium

phosphate mineral found naturally in bone, with chitosan (Ch), a biocompatible natural polymer, results in a scaffold that exhibits properties highly suited for promoting tissue regeneration and cellular proliferation. This scaffold not only supports the growth and

repair of bone tissue but also integrates important mechanical and structural characteristics essential for effective bone regeneration.

To validate the chitosan-Whitlockite scaffold as a suitable material for bone tissue engineering, comprehensive physical, chemical, and biological characterizations are crucial. These include detailed analyses of composition, surface chemistry, mechanical properties, structure, and morphology. The scaffold's ability to support cell proliferation, differentiation, and overall bone repair directly correlates with these characteristics. Studies have consistently demonstrated the importance of these parameters in evaluating scaffolds for tissue engineering applications.

Previous research has shown that WH-based chitosan scaffolds outperform hydroxyapatite (HAP)-chitosan scaffolds in terms of biocompatibility and osteoinductive capacity. For instance, human mesenchymal stem cells (hMSCs) seeded onto WH/Ch scaffolds exhibited enhanced proliferation and differentiation into osteoblasts compared to HAP/Ch scaffolds [28]. This property is particularly important for applications such as calvarial bone repair, where tissue regeneration is critical for successful recovery. Furthermore, the porous structure of the WH/Ch scaffold improves its capacity for tissue integration, providing a favorable environment for cell infiltration and nutrient exchange.

X-ray powder diffraction (XRD) analyzes the scaffold's crystalline structure and provides details on the whitlockite phase composition in the chitosan matrix. The crystalline nature and phase purity of whitlockite are confirmed by the presence of particular diffraction peaks [29]. The whitlockite chitosan scaffold at 3% Wh+Ch sample shows multiple peaks (28.0641°, 31.3816°, 34.7655°) that can be attributed to whitlockite. The 1% Wh+Ch sample also shows characteristic peaks of whitlockite (31.4817°, 46.6158°). However,

the 2% Wh+Ch sample does not show distinct whitlockite peaks, indicating that the whitlockite content is not sufficient to form distinct crystalline phases observable in the XRD pattern. All samples show peaks around 20°, which are characteristic of chitosan. The slight differences in peak positions (20.1965°, 20.845°, 20.6648°) indicate variations in the lattice parameters of chitosan due to different concentrations of whitlockite.

Fourier-transform infrared spectroscopy (FTIR) further confirmed the integration of WH into the chitosan matrix. Characteristic peaks for both chitosan and Whitlockite were identified, with shifts in peak intensity reflecting interactions between the two components. These shifts, particularly in the O-H and N-H stretching regions, suggest the formation of hydrogen bonds between chitosan and phosphate groups from Whitlockite. The preservation of amide, C-H, and P-O stretching bands confirms that the incorporation of Whitlockite did not disrupt the chemical structure of chitosan, supporting the successful formation of a stable composite scaffold. These changes reflect the interactions between chitosan and whitlockite, such as hydrogen bonding, and the incorporation of phosphate groups into the chitosan structure. The consistent presence of amide bands, C-H stretches, and P-O stretches confirms the successful integration of whitlockite into the chitosan matrix [30]. These results fall in accordance with the FTIR spectrum obtained by the Chitosan- whitlockite scaffold. The FTIR for Chitosan-whitlockite scaffold indicates that as the concentration of whitlockite increases in the chitosan matrix, the characteristic peaks of both materials are present, with slight shifts and changes in peak intensity.

Scanning electron microscopy (SEM) provided detailed images of the scaffold's microstructure, revealing a highly porous network with interconnected pores of various sizes. This porous architecture is essential for

facilitating cell infiltration and ensuring adequate nutrient distribution. SEM images also demonstrated that the scaffold's surface morphology, including its rough and fibrous structure, is conducive to cell attachment and proliferation. Energy-dispersive X-ray spectroscopy (EDS) analysis further confirmed the presence of essential elements such as calcium (Ca), phosphorus (P), and magnesium (Mg), which are crucial for bone mineralization and mechanical strength [31].

The scaffold's biocompatibility was evaluated through MTT assays using human osteoblast cells. The results indicated that scaffold concentrations up to 50% did not exhibit cytotoxic effects, with optimal cell viability observed at lower concentrations (25%-50%). These findings are consistent with the general biocompatibility of chitosan and the osteoinductive properties of Whitlockite. Furthermore, the addition of magnesium in the Whitlockite structure enhances osteoblastic activity, promoting bone mineralization. According to estimated cell viability (which ranges from 85% to 130% of control), none of the investigated scaffolds emit harmful chemicals or have an adverse effect on cell activity [32]. The MTT assay was used in the study conducted by [33] to assess the bioactivity of WH particles treated with human osteoblastic cells. During every stage of cell growth, the cell densities in composite scaffolds were consistently higher ($*p < 0.05$) than those in the control group. [34].

The incorporation of Whitlockite into the chitosan matrix not only enhances the scaffold's mechanical strength but also contributes to the bioactive environment necessary for bone regeneration. The mineral content of Whitlockite, particularly calcium and phosphate, plays a pivotal role in promoting bone mineralization and osteoblast activation. Additionally, the magnesium component of Whitlockite contributes to the mechanical stability of newly formed bone tissue, further improving the scaffold's

suitability for bone regeneration applications. The scaffold is a safer alternative for clinical application because of its capacity to inhibit bacterial growth, which can help avoid infections and improve patient outcomes.

The remarkable cell viability and proliferation rates we saw in our assays clearly demonstrated the scaffold's biocompatibility. This implies that the scaffold is a safe choice for medical applications because it does not react negatively with bone cells. Chitosan's acceptability for usage in the body is further supported by its natural origin and capacity to break down into non-toxic components. By boosting the expression of genes linked to calcium binding and mineralization, such as ALP, OPN, and OCN, CS encourages the growth of osteoblasts [35]. Nevertheless, the structure of the scaffold was essential in promoting the formation of bone cells. The chitosan-whitlockite scaffold's porosity structure enables cells to permeate and disperse throughout the substance. This is significant because it allows new bone tissue to grow inside the scaffold, improving integration with the surrounding bone. Whitlockite's presence provides vital minerals including calcium and phosphate, which are necessary for bone mineralization and strength.

The chitosan-Whitlockite scaffold demonstrates significant potential for use in bone tissue engineering and regenerative medicine. Its ability to promote cell proliferation, support tissue regeneration, and offer structural stability makes it an attractive candidate for further research and clinical applications. Future studies should focus on optimizing the scaffold's properties, investigating its performance in various biological environments, and exploring its potential for broader medical applications. With continued research, this scaffold could become a valuable tool for treating bone defects and tissue loss in regenerative medicine.

Conclusion

The biological assessment of the chitosan-Whitlockite (WH) scaffold reveals its substantial potential in tissue engineering and regenerative medicine. The scaffold's ability to support cell adhesion, proliferation, and differentiation makes it a promising material for enhancing tissue growth. Its porous structure facilitates essential cell infiltration and nutrient diffusion, which are critical for tissue regeneration. Chitosan's surface properties further promote cell adhesion, while Whitlockite contributes essential ions, such as calcium and phosphate, crucial for bone cell mineralization and function.

In particular, the scaffold's capacity to foster bone mineralization is of significant value to bone tissue engineering. Magnesium ions in Whitlockite play a pivotal role in promoting bone development and enhancing the mechanical strength of the regenerating tissue. The scaffold effectively stimulates osteoblast activity, leading to the deposition of bone-like minerals, which support tissue regeneration. Additionally, chitosan's inherent

antibacterial properties reduce the risk of infection, which is vital for applications in implants and wound healing. Its biodegradable nature ensures that it naturally degrades into non-toxic byproducts, eliminating the need for surgical removal and allowing for seamless integration within the body.

Overall, the chitosan-Whitlockite scaffold demonstrates a range of favorable biological properties, including bioactivity, biocompatibility, and the ability to support cellular functions essential for tissue regeneration. These findings suggest that the scaffold holds significant promise for applications such as bone grafting, wound healing, and broader tissue engineering efforts. Further studies are warranted to optimize its properties and expand its potential use in various clinical contexts.

Conflict of Interest

Nil.

Acknowledgements

Nil.

References

- [1]. Sheen, J. R., Mabrouk, A., & Garla, V. V., 2023, Fracture Healing Overview. In *StatPearls [Internet]*. StatPearls Publishing. <https://www.ncbi.nlm.nih.gov/books/NBK551678/>
- [2]. Sugumaran, S., Selvam, D., Nivedhitha, M. S., Ganesh Mohanraj, K., Almutairi, B. O., Arokiyaraj, S., Guru, A., & Arockiaraj, J., 2023, Role of individual and combined impact of simvastatin and α -TCP in rat calvarial bone defect: An experimental study. *The Saudi Dental Journal*, 35(7), 861–868. <https://doi.org/10.1016/j.sdentj.2023.07.013>
- [3]. Evaluation of an injectable bioactive borate glass cement to heal bone defects in a rabbit femoral condyle model., 2017, *Materials Science and Engineering: C*, 73, 585–595. <https://doi.org/10.1016/j.msec.2016.12.101>
- [4]. Ye, Y., Pang, Y., Zhang, Z., Wu, C., Jin, J., Su, M., Pan, J., Liu, Y., Chen, L., & Jin, K., 2018, Decellularized periosteum-covered chitosan globule composite for bone regeneration in rabbit femur condyle bone defects. *Macromolecular Bioscience*, 18(9). <https://doi.org/10.1002/mabi.201700424>
- [5]. Shao, R. X., Quan, R. F., Wang, T., Du, W. B., Jia, G. Y., Wang, D., Lv, L. B., Xu, C. Y., Wei, X. C., Wang, J. F., & Yang, D. S., 2018, Effects of a bone graft substitute consisting of porous gradient HA/ZrO₂ and gelatin/chitosan slow-release hydrogel containing BMP-2 and BMSCs on lumbar vertebral defect repair in rhesus monkey. *Journal of Tissue Engineering and*

- Regenerative Medicine*, 12(3).
<https://doi.org/10.1002/term.2601>
- [6]. Vimalraj, S., & Saravanan, S. 2023, Tooth-derived stem cells integrated biomaterials for bone and dental tissue engineering. *Cell and Tissue Research*, 394(2), 245–255. <https://doi.org/10.1007/s00441-023-03815-0>
- [7]. Chitosan-based nanocomposites for the repair of bone defects., 2017, *Nanomedicine: Nanotechnology, Biology, and Medicine*, 13(7), 2231–2240. <https://doi.org/10.1016/j.nano.2017.06.007>
- [8]. Radwan, N. H., Nasr, M., Ishak, R. A. H., Abdeltawab, N. F., & Awad, G. A. S., 2020, Chitosan-calcium phosphate composite scaffolds for control of post-operative osteomyelitis: Fabrication, characterization, and in vitro-in vivo evaluation. *Carbohydrate Polymers*, 244. <https://doi.org/10.1016/j.carbpol.2020.116482>
- [9]. Kumar Dewangan, V., Sampath Kumar, T. S., Doble, M., & Daniel Varghese, V., 2023, Fabrication of injectable antibiotic-loaded apatitic bone cements with prolonged drug delivery for treating post-surgery infections. *Journal of Biomedical Materials Research. Part A*, 111(11), 1750–1767. <https://doi.org/10.1002/jbm.a.37584>
- [10]. Topsakal, A., Uzun, M., Ugar, G., Ozcan, A., Altun, E., Oktar, F. N., Ikram, F., Ozkan, O., Turkoglu, S. H., & Gunduz, O., 2018, Development of Amoxicillin-Loaded Electrospun Polyurethane/Chitosan/ β - Tricalcium Phosphate Scaffold for Bone Tissue Regeneration. *IEEE Transactions on Nanobioscience*, 17(3). <https://doi.org/10.1109/TNB.2018.2844870>
- [11]. *Website*. (n.d.). <https://www.scopus.com/inward/record.url?eid=2-s2.0-85161646526&partnerID=40&md5=2d8d235de025b3474484323088212641>
- [12]. Elakkiya, K., Bargavi, P., & Balakumar, S., 2023, 3D interconnected porous PMMA scaffold integrating with advanced nanostructured CaP-based biomaterials for rapid bone repair and regeneration. *Journal of the Mechanical Behavior of Biomedical Materials*, 147, 106106. <https://doi.org/10.1016/j.jmbbm.2023.106106>
- [13]. Shah, F. A., 2021, Magnesium whitlockite - omnipresent in pathological mineralisation of soft tissues but not a significant inorganic constituent of bone. *Acta Biomaterialia*, 125. <https://doi.org/10.1016/j.actbio.2021.02.021>
- [14]. Batool, S., Liaqat, U., Babar, B., & Hussain, Z., 2021, Bone whitlockite: synthesis, applications, and future prospects. *Journal of the Korean Ceramic Society*, 58(5), 530–547. <https://doi.org/10.1007/s43207-021-00120-w>
- [15]. Batool, S., Liaqat, U., Hussain, Z., & Sohail, M., 2020, Synthesis, characterization and process optimization of bone whitlockite. *Nanomaterials*, 10(9), 1856. <https://doi.org/10.3390/nano10091856>
- [16]. Development and in vivo response of hydroxyapatite/whitlockite from chicken bones as bone substitute using a chitosan membrane for guided bone regeneration, 2018, *Ceramics International*, 44(18), 22583–22591. <https://doi.org/10.1016/j.ceramint.2018.09.032>
- [17]. Kjalarsdóttir, L., Dýrfjörð, A., Dagbjartsson, A., Laxdal, E. H., Örlygsson, G., Gíslason, J., Einarsson, J. M., Ng, C. H., & Jónsson, H., 2019, Bone remodeling effect of a chitosan and calcium phosphate-based composite. *Regenerative Biomaterials*, 6(4). <https://doi.org/10.1093/rb/rbz009>
- [18]. Mickymaray, S., Al Aboody, M. S., Eraqi, M. M., Alhoqail, W. A., Alothaim, A. S., & Suresh, K., 2023, Biopolymer Chitosan surface engineering with magnesium oxide-Pluronic-F127-Escin nanoparticles on human breast carcinoma cell line and microbial strains. *Nanomaterials (Basel, Switzerland)*, 13(7), 1227. <https://doi.org/10.3390/nano13071227>
- [19]. Mickymaray, S., Al Aboody, M. S., Eraqi, M. M., Alhoqail, W. A., Alothaim, A.

- S., Suresh, K., & Arulselvan, P., 2023. Chitosan-encapsulated nickel oxide, tin dioxide, and farnesol nanoparticles: Antimicrobial and anticancer properties in breast cancer cells. *International Journal of Biological Macromolecules*, 248(125799), 125799.
<https://doi.org/10.1016/j.ijbiomac.2023.125799>
- [20]. Website. (n.d.).
<https://www.scopus.com/inward/record.url?eid=2-s2.0-85178134245&partnerID=40&md5=5c28e9476bfefdc06315e3ce2a7b9875>
- [21]. Kazemi Shariat Panahi, H., Dehghani, M., Amiri, H., Guillemin, G. J., Gupta, V. K., Rajaei, A., Yang, Y., Peng, W., Pan, J., Aghbashlo, M., & Tabatabaei, M., 2023, Current and emerging applications of saccharide-modified chitosan: a critical review. *Biotechnology Advances*, 66(108172), 108172.
<https://doi.org/10.1016/j.biotechadv.2023.108172>
- [22]. *Sage Journals: Discover world-class research*. (n.d.). Sage Journals. Retrieved October 4, 2024, from <https://journals.sagepub.com/action/cookieAbsent>
- [23]. Manjubaashini, N., Bargavi, P., Thomas, N. G., Krishnan, N., & Balakumar, S., 2024, Chitosan bioactive glass scaffolds for in vivo subcutaneous implantation, toxicity assessment, and diabetic wound healing upon animal model. *International Journal of Biological Macromolecules*, 256(128291), 128291.
<https://doi.org/10.1016/j.ijbiomac.2023.128291>
- [24]. Hazari, S. A., Sheikh, A., Abourehab, M. A. S., Tullah, A. S., & Kesharwani, P., 2023, Self-assembled Gallic acid loaded lecithin-chitosan hybrid nanostructured gel as a potential tool against imiquimod-induced psoriasis. *Environmental Research*, 234(116562), 116562.
<https://doi.org/10.1016/j.envres.2023.116562>
- [25]. Christina, K., Subbiah, K., Arulraj, P., Krishnan, S. K., & Sathishkumar, P., 2024, A sustainable and eco-friendly approach for environmental and energy management using biopolymers chitosan, lignin and cellulose - A review. *International Journal of Biological Macromolecules*, 257(Pt 2), 128550.
<https://doi.org/10.1016/j.ijbiomac.2023.128550>
- [26]. LogithKumar, R., KeshavNarayan, A., Dhivya, S., Chawla, A., Saravanan, S., & Selvamurugan, N., 2016, A review of chitosan and its derivatives in bone tissue engineering. *Carbohydrate Polymers*, 151.
<https://doi.org/10.1016/j.carbpol.2016.05.049>
- [27]. Tao, F., Cheng, Y., Shi, X., Zheng, H., Du, Y., Xiang, W., & Deng, H., 2020, Applications of chitin and chitosan nanofibers in bone regenerative engineering. *Carbohydrate Polymers*, 230.
<https://doi.org/10.1016/j.carbpol.2019.115658>
- [28]. Zhou, D., Qi, C., Chen, Y.-X., Zhu, Y.-J., Sun, T.-W., Chen, F., & Zhang, C.-Q., 2017, Comparative study of porous hydroxyapatite/chitosan and whitlockite/chitosan scaffolds for bone regeneration in calvarial defects. *International Journal of Nanomedicine*.
<https://www.tandfonline.com/doi/abs/10.2147/IJN.S131251>
- [29]. Xiao, F., Shi, J., Zhang, X., Hu, M., Chen, K., Shen, C., Chen, X., Guo, Y., & Li, Y., 2023, Gadolinium-doped whitlockite/chitosan composite scaffolds with osteogenic activity for bone defect treatment: *In vitro* and *in vivo* evaluations. *Frontiers in Bioengineering and Biotechnology*, 11, 1071692.
<https://doi.org/10.3389/fbioe.2023.1071692>
- [30]. Dissolution-Precipitation Synthesis and Cold Sintering of Mussel Shells-Derived Hydroxyapatite and Hydroxyapatite/Chitosan Composites for Bone Tissue Engineering,

2023, *Open Ceramics*, 15, 100418.
<https://doi.org/10.1016/j.oceram.2023.100418>
[31]. Kowalczyk, P., Podgórski, R.,
Wojasiński, M., Gut, G., Bojar, W., & Ciach,
T., 2021, Chitosan-Human Bone Composite
Granulates for Guided Bone Regeneration.
International Journal of Molecular Sciences,
22(5), 2324.
<https://doi.org/10.3390/ijms22052324>
[32]. Bauer, L., Antunović, M., Gallego-Ferrer,
G., Ivanković, M., & Ivanković, H., 2021,
PCL-Coated Multi-Substituted Calcium
Phosphate Bone Scaffolds with Enhanced
Properties. *Materials*, 14(16), 4403.
<https://doi.org/10.3390/ma14164403>
[33]. Nazurudeen, J., Palati, S., Sekaran, S., &
Ganapathy, D., 2024, Biocompatibility
Evaluation of Ampicillin-Loaded Whitlockite

for Bone Regeneration. *Cureus*, 16(5).
<https://doi.org/10.7759/cureus.61461>
[34]. Investigating the mechanical,
physiochemical and osteogenic properties in
gelatin-chitosan-bioactive nanoceramic
composite scaffolds for bone tissue
regeneration: In vitro and in vivo, 2019,
Materials Science and Engineering: C, 94,
713–728.
<https://doi.org/10.1016/j.msec.2018.10.022>
[35]. Tian, Y., Wu, D., Wu, D., Cui, Y., Ren,
G., Wang, Y., Wang, J., & Peng, C., 2022,
Chitosan-Based Biomaterial Scaffolds for the
Repair of Infected Bone Defects. *Frontiers in
Bioengineering and Biotechnology*, 10,
899760.
<https://doi.org/10.3389/fbioe.2022.899760>